Swiss J Geosci (2013) 106:543–558
DOI 10.1007/s00015-013-0154-4

# Earthquakes in Switzerland and surrounding regions during 2012

**Tobias Diehl · Nicholas Deichmann · John Clinton · Stephan Husen · Toni Kraft · Katrin Plenkers · Benjamin Edwards · Carlo Cauzzi · Clotaire Michel · Philipp Kästli · Stefan Wiemer · Florian Haslinger · Donat Fäh · Urs Kradolfer · Jochen Woessner**

Received: 7 September 2013 / Accepted: 21 October 2013


**Abstract** This report of the Swiss Seismological Service summarizes the seismic activity in Switzerland and surrounding regions during 2012. During this period, 497 earthquakes and 88 quarry blasts were detected and located in the region under consideration. With a total of only 13 events with $M_L \geq 2.5$, the seismic activity in the year 2012 was far below the average over the previous 37 years. Most noteworthy were the earthquake sequence of Filisur (GR) in January with two events of $M_L$ 3.3 and 3.5, the $M_L$ 4.2 and $M_L$ 3.5 earthquakes at a depth of 32 km below Zug in February and the $M_L$ 3.6 event near Vallorcine in October. The epicentral intensity of the $M_L$ 4.2 event close to Zug was IV, with a maximum intensity of V reached in a few areas, probably due to site amplification effects.

**Keywords** Seismicity · Focal mechanisms · Seismotectonics · Zug · Vallorcine

**Zusammenfassung** Dieser Bericht des Schweizerischen Erdbebendienstes stellt eine Zusammenfassung der im Vorjahr in der Schweiz und Umgebung aufgetretenen Erdbeben dar. Im Jahr 2012 wurden im erwähnten Gebiet 497 Erdbeben sowie 88 Sprengungen erfasst und lokalisiert. Mit nur 13 Beben der Magnitude $M_L \geq 2.5$, lag die seismische Aktivität im Jahr 2012 weit unter dem Durchschnitt der vorhergehenden 37 Jahre. Die bedeutendsten Ereignisse waren die Erdbebensequenz von Filisur im Januar mit zwei Beben der Magnitude $M_L$ 3.5 und 3.3, die Beben in 32 km Tiefe bei Zug ($M_L$ 4.2 und $M_L$ 3.5) im Februar sowie das Beben bei Vallorcine ($M_L$ 3.6) im Oktober. Das $M_L$ 4.2 Beben nahe Zug verursachte Erschütterungen der Intensität IV. Sehr vereinzelt wurden Erschütterungen der Intensitäten V verspürt, vermutlich verursacht durch lokale Amplifikationseffekte.

**Resumé** Le présent rapport du Service Sismologique Suisse résume l'activité sismique en Suisse et dans les régions limitrophes au cours de l'année 2012. Durant cette période, 497 tremblements de terre et 88 tirs de carrière ont été détectés et localisés dans la région considérée. Avec seulement 13 événements de magnitude $M_L \geq 2.5$, l'activité sismique de l'année 2012 est bien en-dessous de la moyenne des 37 années précédentes. Les événements les plus significatifs ont été la séquence de Filisur en janvier avec deux séismes de magnitude $M_L$ 3.5 et 3.3, les séismes à une profondeur de 32 km près de Zoug ($M_L$ 4.2 et $M_L$ 3.5) en février et le séisme près de Vallorcine en Octobre ($M_L$ 3.6). L'intensité de l'événement de $M_L$ 4.2 près de Zoug a été de IV, avec une intensité maximale de V atteinte dans quelques zones sans doute en lien avec des effets d'amplification locaux.

Editorial handling: A. G. Milnes.

T. Diehl (✉) · N. Deichmann · J. Clinton · S. Husen · T. Kraft · K. Plenkers · B. Edwards · C. Cauzzi · C. Michel · P. Kästli · S. Wiemer · F. Haslinger · D. Fäh · U. Kradolfer · J. Woessner
Swiss Seismological Service, ETH Zürich, Sonneggstrasse 5, 8092 Zurich, Switzerland
e-mail: tobias.diehl@sed.ethz.ch
URL: http://www.seismo.ethz.ch

## 1 Introduction

Past earthquake activity in and around Switzerland has been documented in an uninterrupted series of annual

reports from 1879 until 1963 (*Jahresberichte des Schweizerischen Erdbebendienstes*). Three additional annual reports have been published for the years 1972–1974. These reports together with historical records of earthquakes dating back to the thirteenth century have been summarized by Pavoni (1977) and provided the basis for the first seismic hazard map of Switzerland (Sägesser and Mayer-Rosa 1978). With the advent of routine data processing by computer, the wealth of data acquired by the nationwide seismograph network has been regularly documented in bulletins with detailed lists of all recorded events (*Monthly Bulletin of the Swiss Seismological Service*). Since 1996, annual reports summarizing the seismic activity in Switzerland and surrounding regions have been published in the present form (Baer et al. 1997, 1999, 2001, 2003, 2005, 2007; Deichmann et al. 1998, 2000a, 2002, 2004, 2006, 2008, 2009, 2010, 2011, 2012). In the course of reassessing the seismic hazard in Switzerland, a uniform earthquake catalogue covering both the historical and instrumental periods was compiled in 2002 (Fäh et al. 2003). The official seismic hazard map of Switzerland based on this catalogue was released in 2004 (Giardini et al. 2004; Wiemer et al. 2009). In 2009, the Earthquake Catalogue of Switzerland was revised (ECOS-09) and is now available on-line (http://www.seismo.ethz.ch/prod/catalog/index). In addition, numerous studies covering different aspects of the recent seismicity of Switzerland have been published in the scientific literature (for overviews and additional references see, e.g. Deichmann 1990; Pavoni and Roth 1990; Rüttener 1995; Rüttener et al. 1996; Pavoni et al. 1997; Deichmann et al. 2000b; Kastrup et al. 2004, 2007; Husen et al. 2007; Marschall et al. 2013).

## 2 Data acquisition and analysis

### 2.1 Seismic stations in operation during 2012

The Swiss Seismological Service (SED) operates two separate nationwide seismic networks, a high-gain predominantly broad-band seismometer network (Table 1) and a low-gain accelerograph network (Table 2). The former is designed to continuously monitor ongoing earthquake activity down to magnitudes well below the human perception threshold, whereas the latter is principally aimed at engineering concerns and thus focuses on recording 'strong motions' in urban areas. In addition, the Seismological Service operates a number of temporary stations for various projects (Table 3). SED stations with on-line data acquisition that were operational at the end of 2012 are shown in Fig. 1.

The broadband station at Emosson dam, EMV, was removed in June 2012 due to construction in the area that has permanently destroyed the vault. A new broadband station in the vicinity is planned once a suitable site is found.

The ongoing densification of the Strong Motion accelerograph network with real-time continuous very-broadband accelerometers (Clinton et al. 2011; Cauzzi and Clinton 2013) continued apace in 2012. The first phase neared completion, with 12 new stations added (SAIG, SALTS, SARK, SBEG, SBRS, SBUH, SIEB, SINS, SMAO, SOLZ, STGK, SZUZ). At SBEG, an analogue accelerometric sensor installed in 1992 was removed. Note that in 2011, the triggered dial-up analogue strong motion hardware at SIOM and SVAM were replaced by real-time digital hardware, a fact not reflected in the 2011 yearly report.

The micro-network setup originally by the SED in 2005 in the region between the Lukmanier Pass and the Leventina Valley was dismantled in 2012. This network monitored an ongoing sequence of earthquakes in the immediate vicinity of the southern segment of the new Gotthard railway tunnel (Husen et al. 2011). The short period stations (and co-located acceleration sensors where installed) at CUNA, CURA, LUKA1, DOETR, RITOM and TONGO were removed. The broadband surface station NALPS at the southern shore of Lai di Nalps continues to run and has been included in the broadband seismic network.

In spring 2012, the ownership of the remaining operational Basel borehole stations that were installed in 2006 to monitor the geothermal energy project was passed from GeoPower Basel Ltd to the Kanton Basel Stadt. Station JOHAN was discontinued during the handover. MATTE and OTER2 are operated by SED under a contract with Kanton Basel Stadt, and complement the existing SED borehole station OTER1.

The earthquakes induced by the geothermal project in Basel have raised concerns about potential seismicity induced by other geothermal projects (even those that do not involve the enhancement of permeability through massive water injections). Therefore, responsible operators have established the practice to include local monitoring capabilities for such projects. The four-station short period array around the southeast tip of Lake Geneva, associated to a project near Noville to drill for natural gas, continued operation through 2012. An array to monitor a geothermal experiment planned for 2012 but delayed to 2013 near Sankt Gallen was installed in January and February 2012 in cooperation with the Sankt Galler Stadtwerke and the Swiss Federal Office of Energy—station SGT00 includes a borehole short period sensor at 205 m depth and a surface accelerometer located beside the drill site. Five additional broadband stations (SGT01, SGT02, SGT03, SGT04 and SGT05) are installed at the surface within a 10 km radius around the borehole landing point (Fig. 1).

A long-term project to monitor seismicity down to magnitude $M_L$ 1.0 across north-eastern Switzerland began

**Table 1** High-gain seismograph stations of the Swiss national network operational at the end of 2012

| Code | Station name | Type |
|---|---|---|
| National on-line network recorded in Zürich | | |
| ACB | Acheberg, AG | EB |
| AIGLE | Aigle, VD | BB |
| BALST | Balsthal, SO | BB |
| BERNI | Bernina, GR | BB |
| BNALP | Bannalpsee, NW | BB, SM |
| BOURR | Bourrignon, JU | BB, SM |
| BRANT | Les Verrières, NE | BB |
| DAVOX | Davos, GR | BB |
| DIX | Grande Dixence, VS | BB, SM |
| EMBD | Embd, VS | BB |
| EWZT2 | Wetzwil, ZH | SP |
| FIESA | Fiescheralp, VS | BB |
| FLACH | Flach, ZH | EB |
| FUORN | Ofenpass, GR | BB |
| FUSIO | Fusio, TI | BB, SM |
| GIMEL | Gimel, VD | BB |
| GRIMS | Grimsel, BE | BB, SM |
| GRYON | Gryon, VS | EB |
| HASLI | Hasliberg, BE | BB |
| LAUCH | Lauchernalp, VS | BB |
| LIENZ | Kamor, SG | BB, SM |
| LKBD | Leukerbad, VS | EB |
| LKBD2 | Leukerbad, VS | SP |
| LLS | Linth-Limmern, GL | BB, SM |
| MMK | Mattmark, VS | BB, SM |
| MUGIO | Muggio, TI | BB |
| MUO | Muotathal, SZ | BB |
| NALPS | Val Nalps, GR | BB |
| PANIX | Pigniu, GR | BB |
| PLONS | Mels, SG | BB |
| SALAN | Lac de Salanfe, VS | EB |
| SENIN | Senin, VS | BB, SM |
| SIMPL | Simplonpass, VS | BB |
| SLE | Schleitheim, SH | BB |
| STEIN | Stein am Rhein, SH | EB |
| SULZ | Cheisacher, AG | BB, SM |
| TORNY | Torny, FR | BB |
| TRULL | Trullikon, ZH | EB |
| VANNI | Vissoie, VS | BB |
| VDL | Valle di Lei, GR | BB, SM |
| WEIN | Weingarten, TG | EB |
| WILA | Wil, SG | BB |
| WIMIS | Wimmis, BE | BB |
| ZUR | Zürich-Degenried, ZH | BB, SM |

Instrument type (all three-component): *SP* 1-s, *EB* 5-s, *BB* broadband, *SM* accelerometer. Signals of LKBD2 are transmitted via analog telemetry

**Table 2** Strong-motion stations of the Swiss national network with on-line data acquisition operational at the end of 2012

| Code | Station name | Type |
|---|---|---|
| On-line strong-motion network | | |
| BIBA | Brigerbad, VS | SM |
| OTTER | Otterbach, BS | SM |
| SAIG | Aigle-Rue de la Gare, VD | SM |
| SALTS | Altdorf-Spital, UR | SM |
| SARK | Sarnen-Kantonsschule, OW | SM |
| SAUR | Augst-Römermuseum, AG | SM |
| SBAF | Basel-Friedhofgasse, BS | SM |
| SBAP | Basel-PUK, BS | SM |
| SBAT | Basel-Tropenhaus, BS | SM |
| SBEG | Bettingen-Gewerbehaus, BS | SM |
| SBIS2 | Binningen, BS | SM |
| SBRS | Brig-Spital, VS | SM |
| SBUA2 | Buchs Kindergarten, SG | SM |
| SBUB | Buchserberg Malbun, SG | SM |
| SBUH | Buchs, Hochschule, SG | SM |
| SCEL | Celerina, GR | SM |
| SCHS | Schaffhausen Spital, SH | SM |
| SCOU | Cournillens, FR | SM |
| SCUC | Scuol-Clozza, GR | SM |
| SCUG | Chur Gewerbeschule, GR | SM |
| SEPFL | Lausanne EPFL, VD | SM |
| SFRA | Frenkendorf, BL | SM |
| SGEV | Genf Feuerwehr, GE | SM |
| SGRA | Grächen-Ausblick, VS | SM |
| SIEB | Sierre-Ecole de Borzuat, VS | SM |
| SINS | Interlaken-Schloss, BE | SM |
| SIOM | Sion-Mayennets, VS | SM |
| SIOO | Sion-Ophtalmologie, VS | SM |
| SIOV | Sion-Valere, VS | SM |
| SKAF | Kaiseraugst-Friedhof, AG | SM |
| SLTM2 | Linthal Matt, GL | SM |
| SLUB | Luzern Bramberg, LU | SM |
| SLUW | Luzern Werkhofstr., LU | SM |
| SMAO | Martigny-Rue d'Octodure, VS | SM |
| SMUK | Muraz-Kläranlage, VS | SM |
| SMUR | Muraz-Reservoir, VS | SM |
| SMZW | Muttenz-Waldhaus, BL | SM |
| SNIB | Sankt Niklaus, VS | SM |
| SOLB | Solothurn Schule Bruhl, SO | SM |
| SOLZ | Solothurn-Zeughausgasse, SO | SM |
| SRER | Reinach Rainenweg, BL | SM |
| SRHB | Riehen-Bäumlihof, BS | SM |
| STAF | Tafers, FR | SM |
| STGK | St. Gallen-Kloster, SG | SM |
| STSP | Tschierv, GR | SM |
| SVAM | Vaz-Muldain, GR | SM |

**Table 2** continued

| Code | Station name | Type |
|---|---|---|
| SVIL | Visp-Litternaring, VS | SM |
| SVIO | Visp-ObereStapfeng., VS | SM |
| SVIT | Visp-Terbinerstr., VS | SM |
| SYVP | Yverdon Rue du Phil, VD | SM |
| SZER | Zernez, GR | SM |
| SZUZ | Zürich, Zeughauswiese, ZH | SM |

Instrument type (all three-component): *SM* accelerometer

in 2011. This project, under a contract with the National Cooperative for the Disposal of Radioactive Waste (Nagra), aims to increase the understanding of seismotectonic processes in the vicinity of proposed sites for deep nuclear waste repositories. In order to reach these goals, the existing network in northern Switzerland and southern Germany is being significantly densified with seven surface stations and three short-period borehole stations at depths of 100–200 m. The additional stations will be in operation for a minimum of 10 years. In 2012, surface stations were installed at BERGE (in Germany) and EMMET; while at STIEG, a 123 m deep short period borehole sensor and a surface accelerometer were installed (Fig. 1). Due to changes in the scope of the project, the station SAIRA in the Swiss Jura was dismantled.

To improve the reliability of locations for events at the periphery or outside of Switzerland, the SED continues to be engaged in an ongoing cross-frontier cooperative effort to exchange seismic data in real-time. The SED continuously records and archives signals from stations in Austria operated by the Zentralanstalt für Meteorologie und Geodynamik in Vienna (ZAMG); in Italy operated by the Istituto Nazionale di Geofisica e Vulcanologia in Rome (INGV), the Istituto di Geofisica, Universita di Genova, the Zivilschutz der Autonomen Provinz Bozen-Südtirol and the Istituto Nazionale di Oceanografia e di Geofisica Sperimentale (OGS) in Trieste; in Germany from the Landeserdbebendienst Baden-Württemberg in Freiburg (LED) and the Bundesanstalt für Geowissenschaften und Rohstoffe in Hannover (BGR); and in France from the Réseau Sismologique et Géodésique Français (RESIF). A total of 35 foreign stations were monitored at the SED in 2012, and the number continues to increase as new high-quality stations come on-line in the border region.

### 2.2 Hypocenter location, magnitude, focal mechanisms and monitoring software

Since the year 2005, hypocenter locations of most of the local earthquakes have been determined using the software package NonLinLoc (Lomax et al. 2000). The P-wave velocity model used was derived from a 3D tomographic inversion of local earthquake data with constraints from controlled source seismics (Husen et al. 2003), and the S-velocities are calculated from the P-velocities using a Vp/Vs ratio of 1.71.

**Table 3** Local seismic networks with on-line data acquisition operational at the end of 2012

| Code | Station name | Type |
|---|---|---|
| *Noville network* | | |
| NOV1 | St. Gingolph, VS | SP |
| NOV2 | Port Valais, VS | SP |
| NOV3 | Caux, VD | SP |
| NOV4 | La tour de Pellz, VD | SP |
| *Basel borehole network* | | |
| MATTE | Schüzenmatte (553) | SP (4.5 Hz) |
| OTER1 | Otterbach (500) | BB, SM |
| OTER2 | Otterbach (2740) | SP (4.5 Hz) |
| *Sankt Gallen network* | | |
| SGT00 | Sennhüslen (SP @ 205) | SP, SM |
| SGT01 | Gaiserwald | BB |
| SGT02 | Zihlschlacht | BB |
| SGT03 | Degersheim | BB |
| SGT04 | Schlatt-Haslen | BB |
| SGT05 | Eggersriet | BB |
| *Nagra network* | | |
| BERGE | Lenzkirch, DE | BB |
| EMMET | Emmethof, AG | BB |
| STIEG | Oberembrach-Stiegenhof, ZH (SP @ 123) | SP(4.5 Hz), SM |

Instrument type (all three-component): *SP* 1-second, unless otherwise indicated, *BB* broad-band, *SM* accelerometer. The numbers in parentheses next to the borehole stations are the sensor depth with respect to ground surface in meters

Local magnitudes ($M_L$) are calculated from the maximum amplitude of the horizontal components of the digital broad-band seismograms filtered to simulate the response of a Wood-Anderson seismograph. The attenuation with epicentral distance is accounted for by an empirically determined relation (Kradolfer and Mayer-Rosa, 1988). The final magnitude corresponds to the median value of all individual station magnitudes. For the stronger events, the traditional determination of focal mechanisms from the azimuthal distribution of first-motion polarities (fault-plane solutions) is complemented by moment tensors based on full-waveform inversion. This procedure, based on a time domain inversion scheme developed by Dreger (2003), also provides a moment magnitude, $M_W$, the best fitting double couple, and an optimal depth estimate based on the given location. An additional procedure has been implemented that routinely and automatically provides estimates of $M_W$ also for earthquakes of lower magnitudes. $M_W$ values are

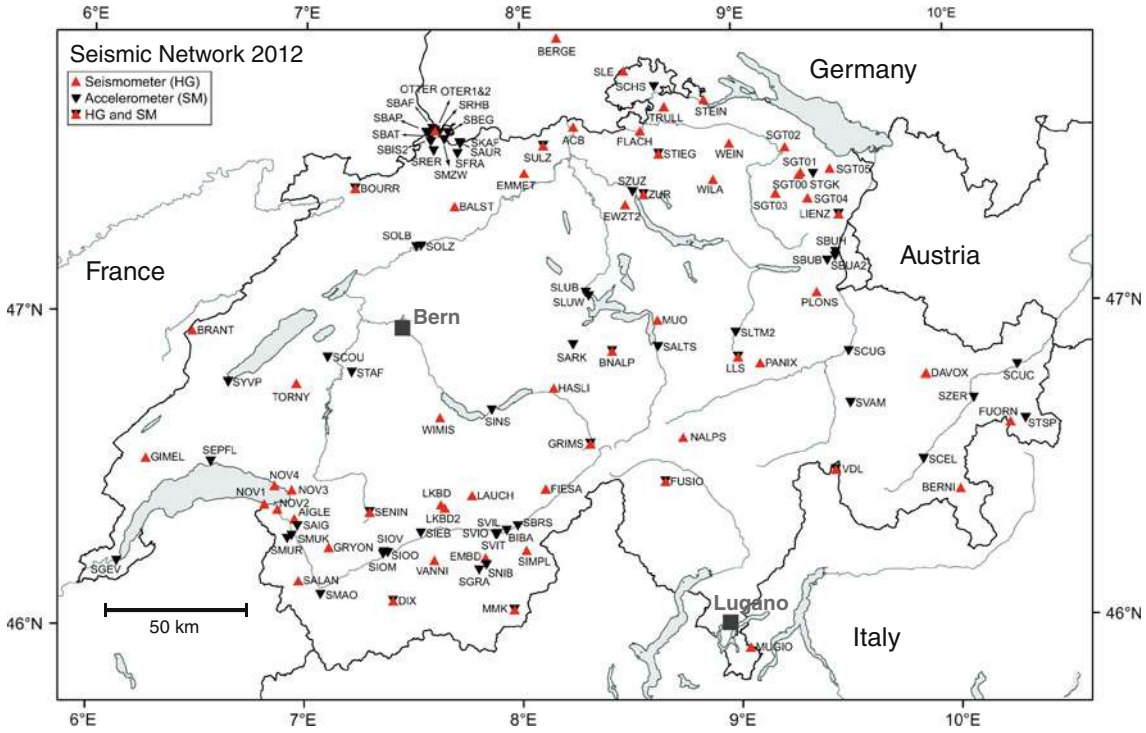


**Fig. 1** Seismograph stations in Switzerland with on-line data acquisition operational at the end of 2012. The stations defined as high-gain (HG) are mostly equipped with broad-band or 5-second sensors, whereas the strong-motion stations (SM) are accelerometers (see also Tables 1, 2, 3)

computed using a spectral fitting technique following the method of Edwards et al. (2010). The far-field signal moments are obtained by simultaneously fitting the spectrum of a theoretical source model (Brune 1970, 1971) along with path variable attenuation and event stress-drop to observed Fourier velocity spectra. The seismic moment is derived from the far-field signal moments assuming a simple geometrical spreading model that accounts for body and surface wave propagation. Site amplification is derived for the whole network following the approach detailed in Edwards et al. (2013). Using this information all data are corrected to a reference hard-rock recording site (Poggi et al. 2011) before computing $M_W$.

A more detailed documentation of the data analysis can be found in previous annual reports (Deichmann et al. 2006; Baer et al. 2007).

In October 2012, the Seismic Network migrated to a new software suite for automatic earthquake detection and characterization as well as manual event review and catalogue management. This software, SeisComP3 (Hanka et al. 2010; http://www.seiscomp3.org), is an open source, community supported tool developed at the GeoForschungsZentrum Potsdam. During a development and testing period lasting several years, all critical features from the previous internally developed software have been included in SeisComp3. This includes the Baer-Kradolfer automated picker (Baer and Kradolfer 1987), the Swiss Local magnitude relationship (Kradolfer and Mayer-Rosa 1988), the NonLinLoc earthquake location algorithm (Lomax et al. 2000), and all relevant velocity models (e.g. Husen et al. 2003). The extensive development and testing ensured that there is no change in the detection threshold of earthquakes and the location accuracy of the reviewed catalogue remains the same. Additionally, there is no systematic bias introduced to the magnitude estimation. SeisComP3 provides a modern software framework with an extensible modular structure, and we expect that the network will use this software for the foreseeable future.

## 3 Seismic activity during 2012

### 3.1 Overview

During 2012, the Swiss Seismological Service detected and located 497 earthquakes in the region shown in Fig. 2. Based on criteria such as the time of occurrence, the location, signal character or on direct communication, 88 additional seismic events were identified as quarry blasts.

Magnitude values of the events recorded in 2012 range from $M_L$ 0.0 to 4.2 (Fig. 3). The events with $M_L \geq 2.5$ and the criteria used to assign the quality rating for the given locations as well as the corresponding estimated location accuracy are listed in Tables 4 and 5. Table 4 also includes the available $M_w$ values derived from the spectral fitting method of Edwards et al. (2010) and from method of

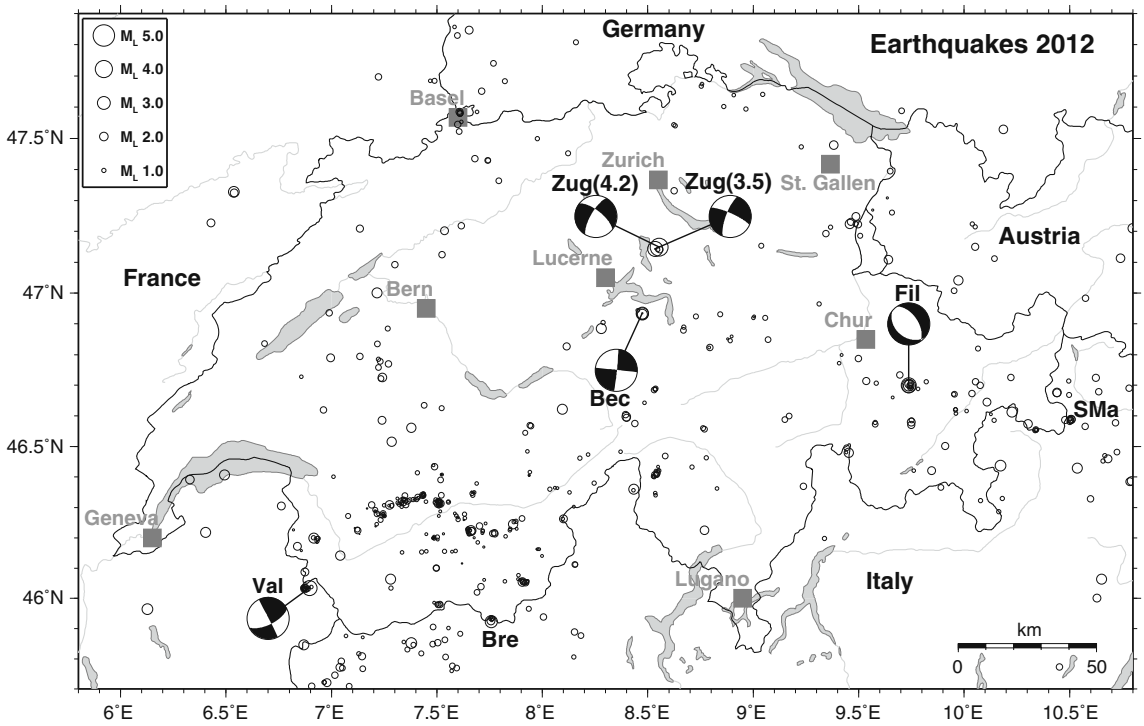


**Fig. 2** Epicenters and focal mechanisms of earthquakes recorded by the Swiss Seismological Service during 2012. Epicenters of events mentioned in the text are Beckenried (Bec), Breithorn (Bre), Filisur (Fil), Santa Maria (SMa), Vallorcine (Val), and Zug (Zug)

Dreger (2003) when available. Fault-plane solutions based on first-motion polarities are shown in Fig. 4 (see also Fig. 2) and their parameters are listed in Table 6.

Figure 5 shows the epicenters of the 893 earthquakes with $M_L \geq 2.5$, which have been recorded in Switzerland and surrounding regions over the period 1975–2012. These events represent about 7 % of the total number of events detected during that time period in the same area. The chosen magnitude threshold of $M_L$ 2.5 ensures that the data set is complete for the given period (Nanjo et al. 2010) and that the number of unidentified quarry blasts and of badly mislocated epicenters is negligible.

## 3.2 Significant earthquakes of 2012

### *3.2.1 Filisur*

On January 1st and 2nd, 2012, two moderate earthquakes with $M_L$ 3.3 and 3.5 jolted the central parts of Kanton Graubünden. They were part of a sequence of nine events that occurred over 3 days with epicenters about 5 km east-northeast of Filisur (Marschall et al. 2013). The $M_L$ 3.5 event was felt in the part of the Graubünden and maximum intensities of IV have been reported. With the closest station 14 km away (DAVOX), routinely computed focal depths are uncertain, and individual events scatter between 2 and 8 km, depending on the number of available arrivals. A comparison of the arrival-time differences between the reflection at the Moho (PmP) and the direct arrival (Pg) observed for the mainshock of this sequence at stations WILA and ZUR with those of one of the events of the Sertig sequence of 2003, located 8 km further to the east-northeast, shows that the source of the Filisur sequence was slightly shallower than the Sertig sequence (Fig. 6). Since the focal depth of the Sertig sequence (7 km) is well constrained by records of a temporary station installed in the immediate vicinity of the epicenter (Deichmann et al. 2004), we conclude that the hypocenters of the Filisur sequence are located at a depth of about 6 km. This was confirmed by 2D ray-trace modeling of the Pg and PmP travel times observed at several stations in northern Switzerland.

The fault-plane solution computed for the $M_L$ 3.5 event (Table 6; Fig. 4) is based on take-off angles derived from the 2D ray-tracing assuming a linear velocity gradient between the base of the near-surface sediments and the Moho. The result is a normal-faulting focal mechanism with a NE–SW oriented T-axis, typical for this region (e.g. Marschall et al. 2013; Kastrup et al. 2004).

Judging from the high degree of similarity between the waveforms from the individual events in the sequence, the hypocenters must be closely co-located and their focal mechanisms nearly identical. To discriminate between the two nodal planes, a good constraint of the relative focal depths is essential. Given the large epicentral distance of the closest stations, this requires the inclusion of the PmP

arrivals observed at stations in northern Switzerland in the cross-correlation. As a consequence, relative locations could be computed only for the three strongest events (Marschall et al. 2013). Mean travel-time residuals of the relative locations are between 2 and 3 ms, and the resulting location errors (one standard deviation) are on the order of 10 m horizontally and 23 m vertically. Within the location errors, the nodal plane dipping to the SW best matches the vertical distribution of the three hypocenters (Marschall et al. 2013).

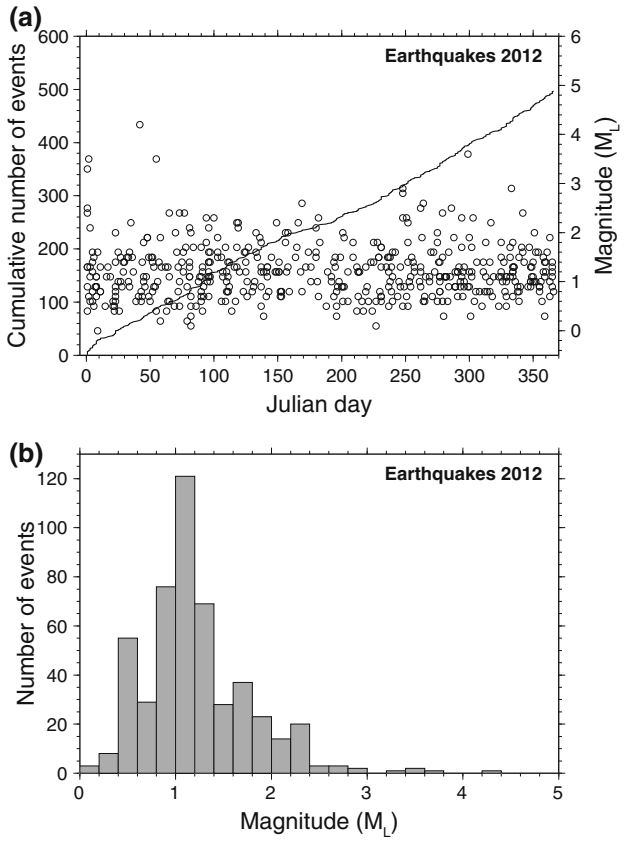


**Fig. 3** Earthquake activity during 2012: **a** magnitude of each event and cumulative number of events; **b** histogram of magnitudes

### *3.2.2 Zug*

The $M_L$ 4.2 earthquake that occurred on February 11th at 11:45 pm local time (10:45 pm UTC) between Zuger- and Ägerisee, was the strongest earthquake to occur in Switzerland since the $M_L$ 4.3 earthquake of Fribourg in 1999 and the $M_L$ 4.9 Vallorcine earthquake in 2005, which was located just across the border with France, between Martigny and Chamonix. The hypocentral depth of 32 km is well constrained by P- and S-onsets at seven stations at epicentral distances between 20 and 40 km. According to the recently published crustal model of the Alps of Wagner et al. (2012), the Moho lies at a depth of about 34 km at this location (Fig. 7). Thus, the $M_L$ 4.2 earthquake locates close to a previously known group of lower-crustal events in the area between the lakes of Zürich and Zug discussed in previous reports (e.g. Deichmann 1992; Deichmann et al. 2000a). Figure 8 shows a record section along a WSW trending profile of an $M_L$ 3.5 aftershock with an almost identical hypocenter location at 32 km depth. In this direction the apparent velocity of the Pn arrivals is 8.15 km/s, while for the Pg arrivals beyond 80 km it is approximately 6.2 km/s. The unusually small Pn–Pg cross-over distance of about 70 km is evidence for the close proximity of the hypocenter to the Moho.

**Table 4** Earthquakes with $M_L \geq 2.5$

| Date and time UTC | Lat. (°N) | Lon. (°E) | X/Y (km) | Z (km) | Mag. ($M_L$) | Mag. ($M_W$) | Mag. ($M_{WSPEC}$) | Q | Location |
|---|---|---|---|---|---|---|---|---|---|
| 2012/01/01 15:33:49 | 46.698 | 9.737 | 776/174 | 8 | 3.3 | – | 3.0 | A | Filisur, GR |
| 2012/01/01 17:16:57 | 46.699 | 9.737 | 776/174 | 7 | 2.5 | – | 2.5 | A | Filisur, GR |
| 2012/01/02 01:42:57 | 46.700 | 9.737 | 776/175 | 8 | 3.5 | – | 3.2 | A | Filisur, GR |
| 2012/02/11 22:45:26 | 47.149 | 8.553 | 684/222 | 32 | 4.2 | 3.7 | 3.8 | A | Zug, ZG |
| 2012/02/24 00:32:29 | 47.144 | 8.534 | 683/222 | 32 | 3.5 | – | 3.0 | A | Zug. ZG |
| 2012/06/17 11:20:38 | 45.965 | 6.126 | 498/091 | 9 | 2.6 | – | 2.6 | D | Annecy, F |
| 2012/09/04 02:51:44 | 46.933 | 8.474 | 679/198 | 9 | 2.8 | – | 2.7 | A | Beckenried, NW |
| 2012/09/04 05:13:24 | 46.935 | 8.474 | 679/199 | 9 | 2.9 | – | 2.8 | A | Beckenried, NW |
| 2012/09/18 23:43:12 | 47.328 | 6.536 | 532/242 | 1 | 2.5 | – | 2.6 | C | Chazot, F |
| 2012/09/20 07:59:05 | 46.438 | 10.173 | 810/146 | 8 | 2.6 | – | 2.4 | A | Val Viola, I |
| 2012/10/12 20:41:32 | 45.853 | 7.378 | 595/078 | 7 | 2.5 | – | 2.5 | B | Valpelline, I |
| 2012/10/25 01:10:57 | 46.035 | 6.896 | 558/098 | 4 | 3.6 | 3.3 | 3.3 | A | Vallorcine, F |
| 2012/11/28 13:32:50 | 45.924 | 7.758 | 625/086 | 2 | 2.9 | – | 2.9 | B | Breithorn, I |

The values listed under $M_W$ are moment magnitudes derived from the moment tensor inversion shown in Fig. 4. The values listed under $M_{WSPEC}$ are the moment magnitudes calculated from the spectral fitting method documented in Edwards et al. (2010). The quality rating (Q) is defined in Table 5. The focal depths of the Filisur and Vallorcine events are constrained by the additional analysis of PmP phases as described in the text

The well-constrained fault-plane solution corresponds to a strike-slip mechanism with a minor component of normal-faulting (Table 6; Fig. 4). In agreement with other known focal mechanisms in this region, its P-axis trends towards NNW–SSE (Kastrup et al. 2004). In the 2 weeks following the February 11th mainshock, 3 aftershocks were recorded with similar locations and depths. A $M_L$ 1.1 event occurred at 28 km depth on February 14th, followed by a $M_L$ 1.6 event at 29 km depth on February 18th. A larger aftershock of $M_L$ 3.5 occurred at 32 km depth on February 24th. The well-constrained fault-plane solution of this event is similar but not identical to that derived for the mainshock (Table 6; Fig. 4).

**Table 5** Criteria and location uncertainty corresponding to the quality rating (Q) of the hypocentral parameters in the event list in Table 4

| Rating | Criteria | | Uncertainty | |
|---|---|---|---|---|
| Q | GAP (°) | DM (km) | H (km) | Z (km) |
| A | ≤180 | ≤1.5 × Z | ≤2 | ≤3 |
| B | ≤200 | ≤25 | ≤5 | ≤10 |
| C | ≤270 | ≤60 | ≤10 | >10 |
| D | >270 | >60 | >10 | >10 |

*GAP* largest angle between epicenter and two adjacent stations, *DM* minimum epicentral distance, *H* horizontal location, *Z* focal depth

The $M_L$ 4.2 mainshock was felt throughout Switzerland, and was widely felt in the eastern and central Alpine foreland, spreading to the eastern extensions of the Jura to the Basel area and to the Lake of Constance (Fig. 9a). Significantly fewer reports were received from the southern and western parts of Switzerland and the Alpine area as a whole, which is even more evident in the distribution of intensities of the $M_L$ 3.5 aftershock (Fig. 9b). The epicentral intensity on the European Macroseismic Scale (EMS) of the mainshock was IV, with a relatively "flat"

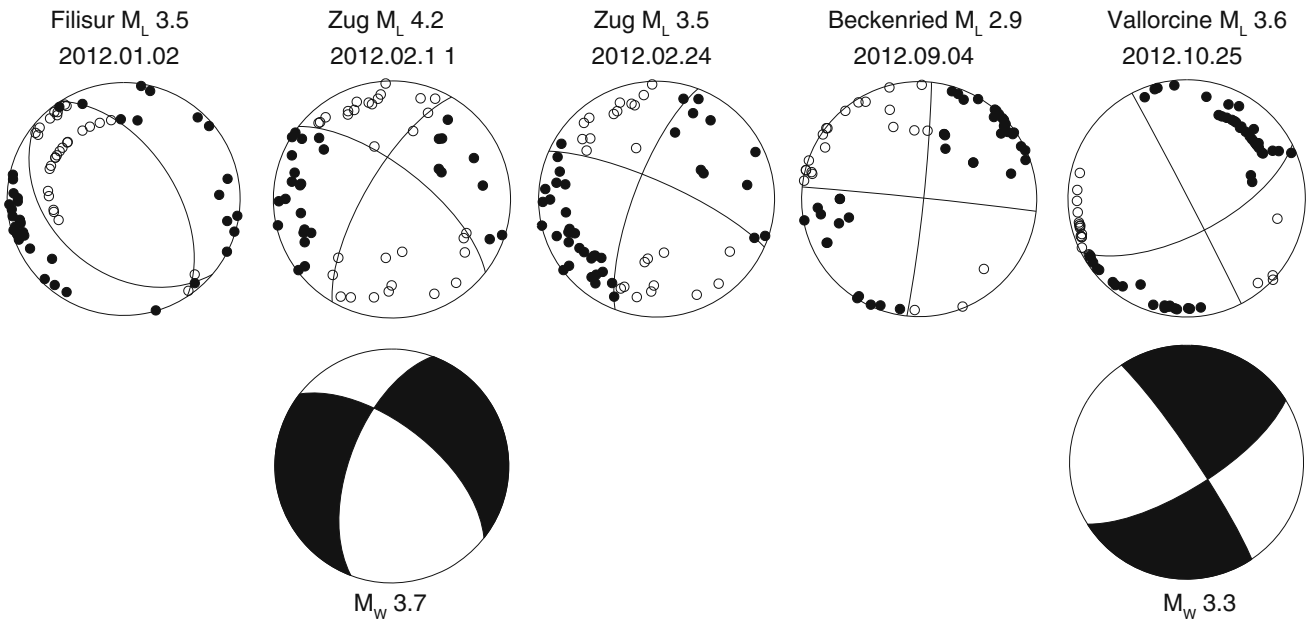


**Fig. 4** Fault-plane solutions based on first-motion polarities (see Table 6). All stereographs are lower hemisphere, equal-area projections. *Solid circles* correspond to compressive first motion (*up*); *empty circles* correspond to dilatational first motion (*down*). Full waveform moment tensor solutions are shown as *beach-ball symbols* for the two largest events where high quality fits are obtained

**Table 6** Focal mechanism parameters based on first-motion polarities of five earthquakes in 2012

| Location | Date and time UTC | Depth (km) | Mag. | Plane 1 Strike/Dip/Rake | Plane 2 Strike/Dip/Rake | P-axis Azimuth/Plunge | T-axis Azimuth/Plunge |
|---|---|---|---|---|---|---|---|
| Filisur | 2012/01/02 01:42:57 | 8 | 3.5 | 327/54/−080 | 130/37/−103 | 274/78 | 050/08 |
| Zug | 2012/02/11 22:45:26 | 32 | 4.2 | 308/68/−160 | 210/72/−023 | 168/29 | 260/02 |
| Zug | 2012/02/24 00:32:29 | 32 | 3.5 | 294/78/−164 | 201/74/−012 | 158/20 | 067/03 |
| Beckenried | 2012/09/04 05:13:24 | 9 | 2.9 | 006/87/001 | 276/89/177 | 321/01 | 231/03 |
| Vallorcine | 2012/10/25 01:10:57 | 4 | 3.6 | 063/65/−179 | 333/89/−025 | 285/18 | 021/17 |

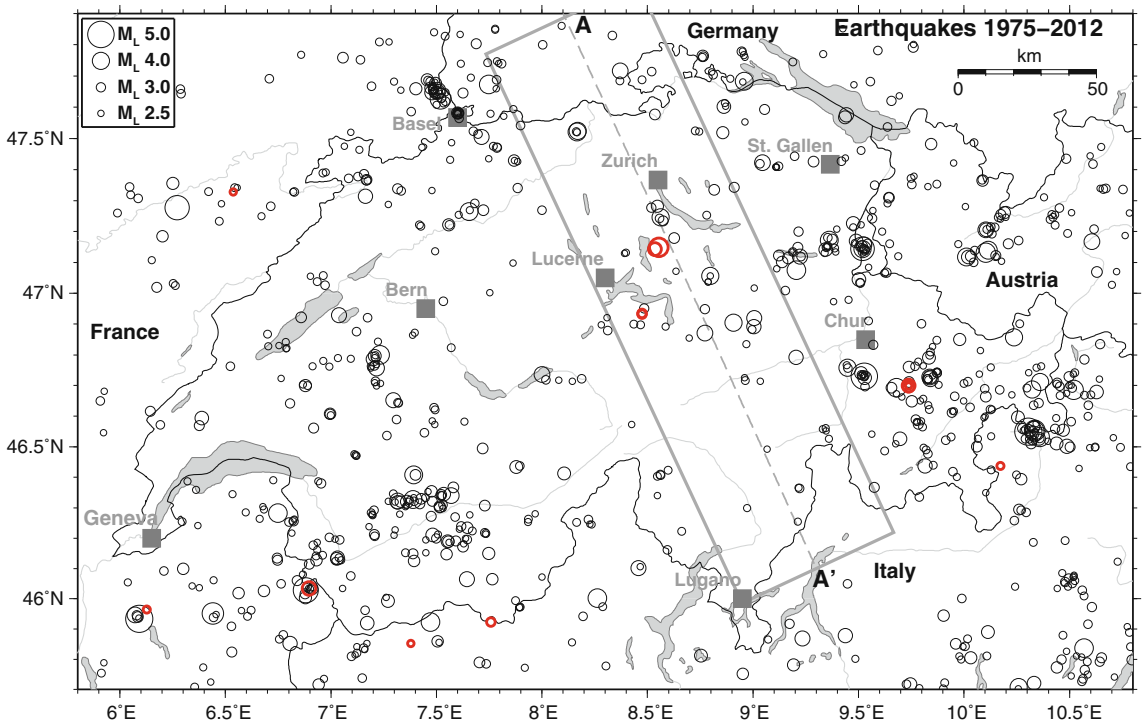


**Fig. 5** Epicenters of earthquakes with magnitudes $M_L \geq 2.5$, during the period 1975–2012. *Grey circles* denote earthquakes in the period 1975–2011, *bold red circles* indicate earthquakes in 2012. The *grey dashed line* and the *solid grey box* mark the location of the profile A–A′ shown in Fig. 7

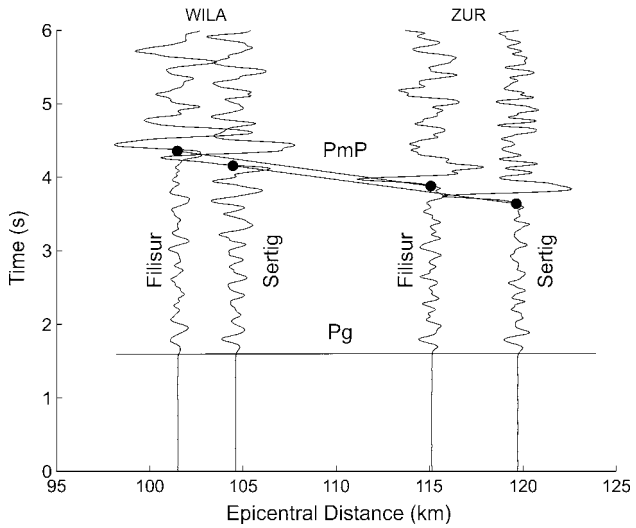


**Fig. 6** Comparison of the PmP arrivals at stations WILA and ZUR of an event of the Sertig sequence (2003/07/18 11:01, $M_L$ 3.9) and of the Filisur sequence (2012/01/02 01:42, $M_L$ 3.5). The signals are integrated to displacement with a Wood-Anderson filter and filtered with a 1–20 Hz, 2nd order Butterworth band-pass filter

intensity field typical for deep events. The maximum intensity of V has been reported in a few areas, probably due to site amplification effects (Fig. 9a).

Figure 10 shows the ground motion recordings of the $M_L$ 4.2 mainshock at two stations of the Swiss National Strong Motion Network (SSMNet) installed in Lucerne about 21 km from the epicenter. Station SLUB (Bramberg) is a rock site on a hill above the city center. Station SLUW is located in the deep basin of Lucerne, near the main train station. The recordings at SLUB show an impulsive, unilateral signal pulse of the S-phase, with a peak displacement of 0.07 mm. The recordings at station SLUW show long-lasting reverberations due to local site effects and the peak displacement is amplified by a factor of 2 compared to the rock site.

### 3.2.3 Beckenried

On September 4th three earthquakes with $M_L$ 2.3, 2.8, and 2.9 occurred within 4 h near Beckenried on the southern shore of the Vierwaldstättersee. The events are located close to the epicenter of the $M_L$ 3.0 earthquake of 2000 (Baer et al. 2001). The high similarity between the signals of the three events of 2012 (Figs. 11, 12) suggests that the hypocenters must be co-located and their focal mechanisms nearly identical. The epicenter location of the 2000 event is located 2–3 km north-northeast of the others, which is in agreement with the difference in S–P times observed at station BNALP (located to the south of the epicenters) shown in Fig. 11.

The focal depths of the 2012 $M_L$ 2.8 and 2.9 events are constrained by P- and S-arrivals at stations BNALP and

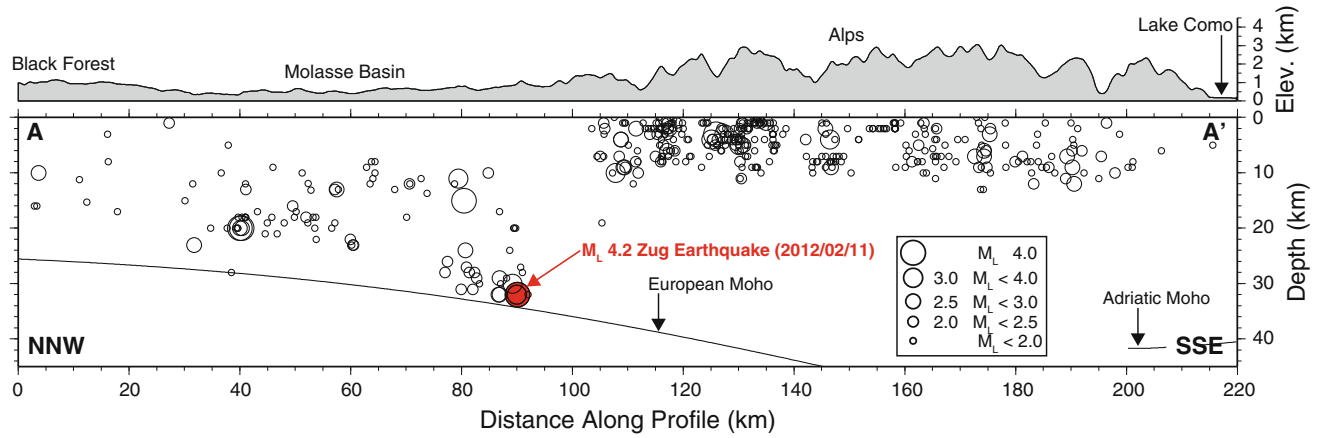


**Fig. 7** Depth cross-section from the Black Forest to Lake Como (see Fig. 5 for location of profile) showing seismicity from 1984 to 2012 (*circles*) as recorded by the SED. The $M_L$ 4.2 mainshock of February 11, 2012 is marked as a *red dot*. Only earthquakes within a swath of ±30 km of the profile (see *box* in Fig. 5) and with well constrained focal depths (i.e. azimuthal GAP ≤180°, number of observations ≥11, distance to closest station ≤30 km) are shown. These selection criteria are the same as those used for earlier compilations of focal depths (e.g. Deichmann et al. 2000a). Size of the *circles* is scaled by magnitude, as indicated. Crust–mantle boundary (Moho) from Wagner et al. (2012) along profile is shown as *black line*

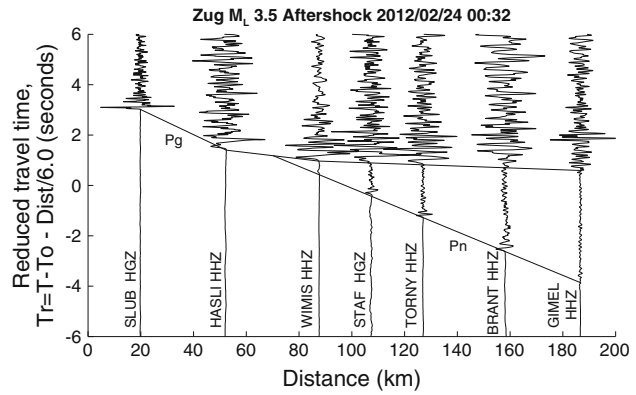


**Fig. 8** Record section of the seismograms of the $M_L$ 3.5 Zug event of 2012/02/24 00:32 as a function of epicentral distance along a WSW trending profile. The signals are filtered with a 0.5–10 Hz Butterworth band-pass filter. In this direction, the apparent velocity of the Pn arrivals is 8.15 km/s and for the Pg arrivals beyond 80 km it is approximately 6.2 km/s. The unusually small Pn–Pg cross-over distance of about 70 km is evidence for the close proximity of the hypocenter to the Moho

MUO at 8 and 13 km epicentral distance as well as by several Pn arrivals (stations KIZ, GUT, UBR and BRANT). At 9–10 km depth, these events are most likely located in the basement. This differentiates them from most of the other well-located events in central Switzerland, which occurred in the overlying sedimentary units (Deichmann et al. 2000b). Assuming a constant seismic velocity ratio (Vp/Vs) for the entire crystalline crust, the observed arrival-time differences between Pg, PmP and Sg, SmS at station SGT04 (Fig. 12) gives Vp/Vs = 1.73 ± 0.03.

The focal mechanism of the $M_L$ 2.9 2012 event (Table 6; Fig. 4) is very similar to the one of 2000: strike-slip with more or less N–S and E–W trending nodal planes. The focal mechanisms of the $M_L$ 2.9 and the $M_L$ 2.8 events (not shown) are actually identical, as expected from the almost identical signals. The fault-plane solution of the $M_L$ 2.3 event (not shown) is not well constrained, but it shows that the focal mechanism is not identical to that of the other events. This is also consistent with the differences in S/P amplitude ratios visible for station BNALP (less nodal) in Fig. 11. The orientation of the P- and T-axes is typical for earthquakes in central Switzerland (e.g. Kastrup et al. 2004).

### 3.2.4 *Vallorcine*

The $M_L$ 3.6 earthquake that occurred on October 25th close to the village of Vallorcine (France) is part of the ongoing earthquake sequence that followed the $M_L$ 4.9 earthquake of September 2005 (Fréchet et al. 2010). The $M_L$ 3.6 event of October 2012 was the strongest earthquake in the region since the September 2005 mainshock. The 2012 event was felt in the southwestern part of the Valais and maximum intensities of IV have been reported. The routine epicenter location of the event is within the main cluster of activity, labeled C1 in the study of Fréchet et al. (2010).

The routinely computed focal depth of 11 km derived from using all available P-wave arrivals (71) is not consistent with focal depths computed for past seismicity of the Vallorcine sequence, including the $M_L$ 4.9 2005 earthquake, despite the fact that this focal depth estimate is well constrained by the large number of Pg and Pn arrivals. Using only Pg- and Sg-wave arrivals up to 80 km distance yields a focal depth of 4 km, which is consistent with focal depths for past seismicity of the Vallorcine sequence. Due to the lack of observations at close distances and of Pn

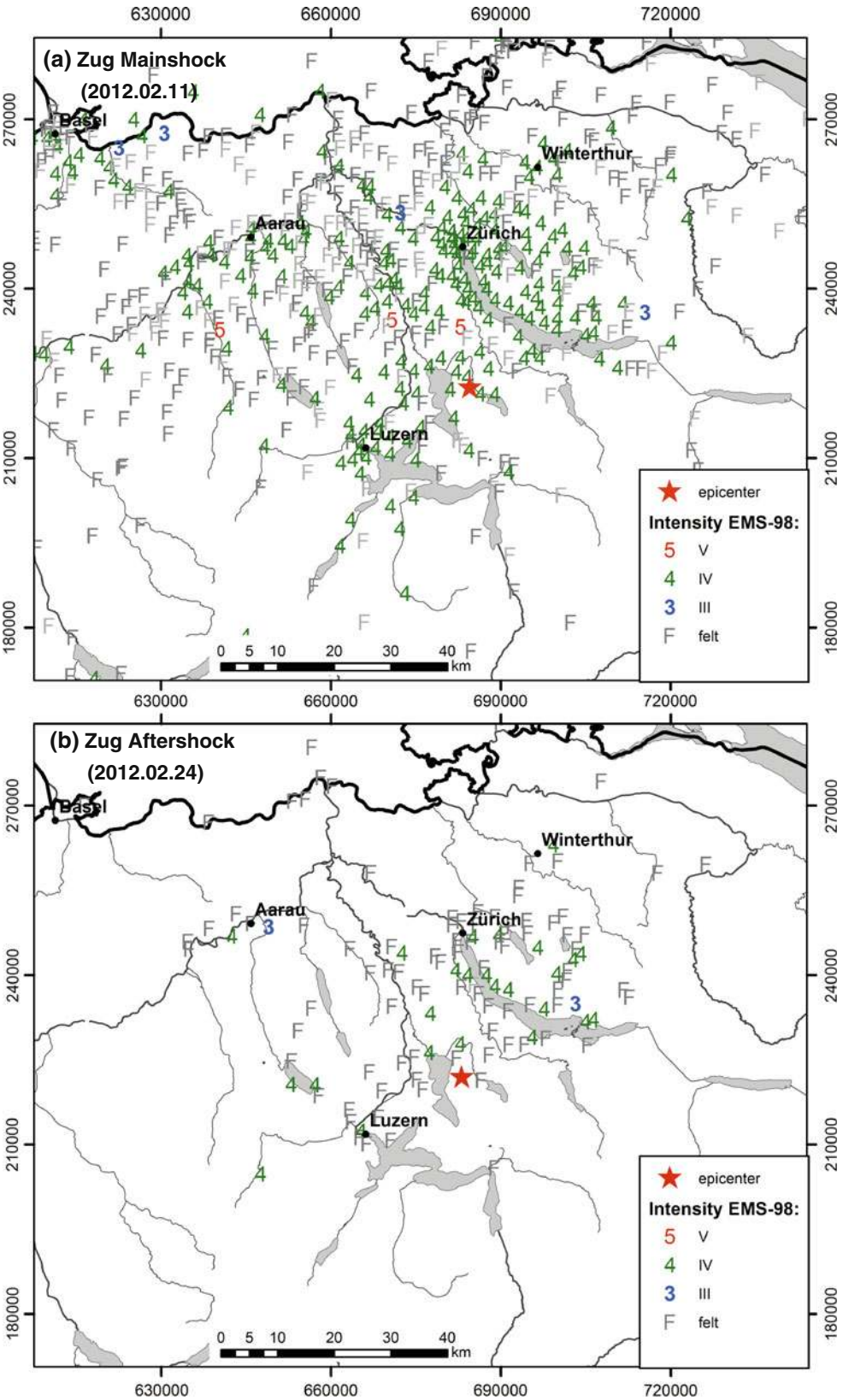


**Fig. 9** Macroseismic intensities (EMS-98) of **a** the $M_L$ 4.2 Zug mainshock of February 11 and **b** the strongest aftershock with $M_L$ 3.5 of February 24

arrivals at large distances this focal depth estimate is not well constrained (uncertainty of ±3.0 km). A focal depth of 4 km yields large negative travel time residuals (>1 s) for Pn arrivals at larger distances but smaller travel time residuals for nearby stations OGSI (RESIF) and SALAN. This suggests that a focal depth of 4 km is more consistent

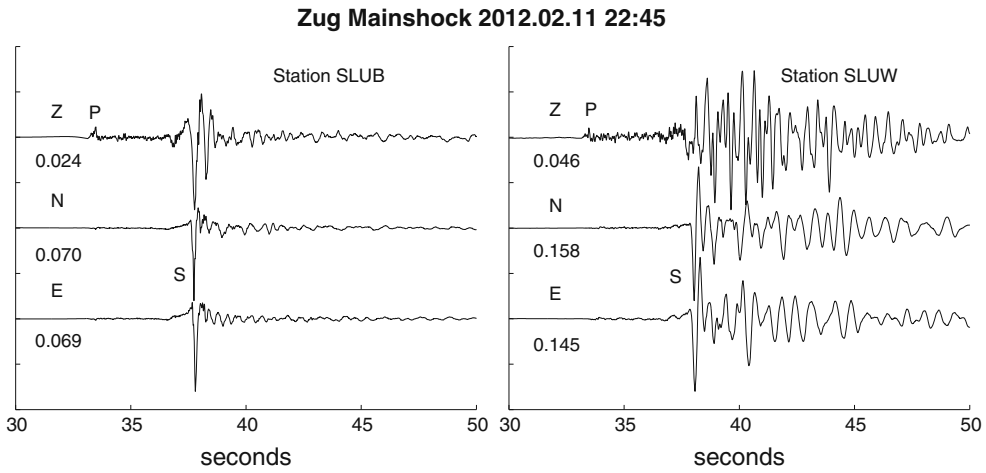


**Fig. 10** Displacement seismograms of the $M_L$ 4.2 earthquake of Zug recorded at two accelerographs in the city of Lucerne. Epicentral distance to both stations is about 21 km, distance between stations is about 1.6 km. To stabilize the double integration of the original accelerograms, the signals where filtered with a 0.5 Hz, 4th order, zero-phase high-pass Butterworth filter and detrended with a second order polynomial. Note the impulsive unilateral signal pulse of the S-phase on the two horizontal components at station SLUB (*right*), situated on hard rock, compared to the long duration reverberations of the S-phase at station SLUW (*left*), situated on unconsolidated sediments near the lake shore. Note also the amplification by a factor of 2 of the peak displacement (given below each trace in mm) at station SLUW compared to station SLUB

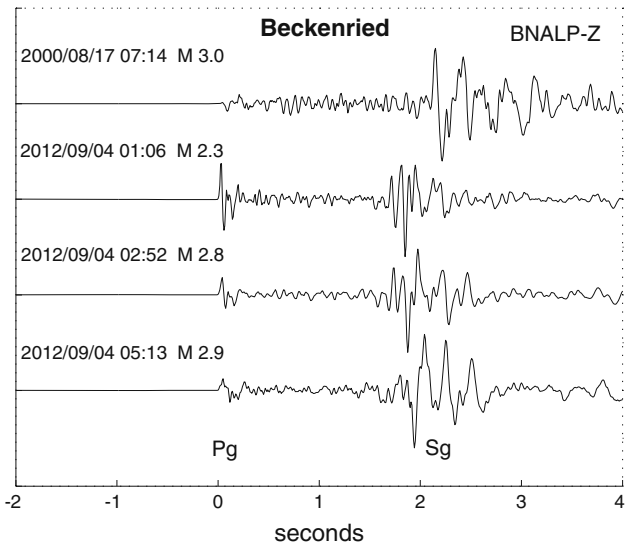


**Fig. 11** Vertical component seismograms recorded at station BNALP of the $M_L$ 3.0 Beckenried event of the year 2000 compared to the three Beckenried events of 2012 at epicentral distances of about 8 km. Note the larger S–P travel-time difference for the event of 2000, which is compatible with the calculated location difference between the hypocenter of this event and that of the three events of 2012. Note also the significantly larger P/S amplitude ratio of the first event of 2012 compared to that of the subsequent two events, which is indicative of a slightly different focal mechanism

with observations at nearby stations but that a focal depth of 11 km is more consistent with distant Pn arrivals. Hypocenter locations were computed using a 3-D P-wave velocity model of Husen et al. (2003), which includes a priori information on Moho depths beneath Switzerland and surrounding regions. This model, however, shows a relatively broad velocity gradient across the Moho instead of a rather sharp velocity gradient, which would be more realistic. Consequently, Pn arrivals are traced as diving waves in the model of Husen et al. (2003), which may lead to longer ray paths when compared to those computed in a model with a sharp velocity gradient across the Moho. Longer ray paths yield larger theoretical travel times and, hence, negative travel time residuals as observed.

Waveforms recorded at station AIGLE for the strongest aftershock ($M_L$ 3.0) of the $M_L$ 4.9 2005 Vallorcine earthquake and the $M_L$ 3.6 2012 earthquake show nearly identical S–P times (Fig. 13). This suggests that the $M_L$ 3.6 2012 earthquake occurred close to strongest aftershock of the $M_L$ 4.9 2005 earthquake, consistent with the obtained epicenter location. PmP arrival times of the strongest aftershock and the $M_L$ 3.6 2012 earthquake at station TORNY are very similar (Fig. 13). This suggests that both events occurred at a similar focal depth. Given the uncertainty in computing correct Pn ray paths, as discussed above, and a focal depth of 4 km for the aftershock constrained by a densely spaced deployment in September 2005 (Fréchet et al. 2010), a focal depth of 4 km for the $M_L$ 3.6 2012 Vallorcine earthquake seems more plausible.

The focal mechanism derived from the analysis of first-motion polarities of the $M_L$ 3.6 event (Table 6; Fig. 4) is almost identical with the mechanism of the 2005 mainshock published by Fréchet et al. (2010). The high similarity of waveforms to the 2005 aftershock and the similarity in the focal mechanisms suggest that, like in the 2005 mainshock, the plane striking N63°E was active in the 2012 event.

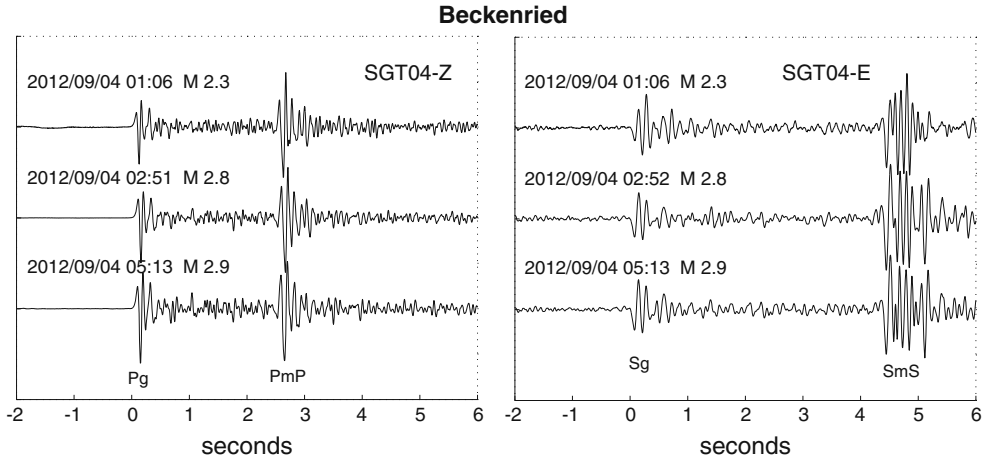


**Fig. 12** Seismograms (ground velocity; 0.5 Hz, 4th order, zero-phase Butterworth high-pass filter) of the three Beckenried events of 2012 recorded at station SGT04 (epicentral distance 81 km). The vertical components (*left panel*) are aligned on the Pg arrival; the E–W components (*right panel*) are aligned on the Sg arrival. Note the almost identical travel-time differences between the reflections at the Moho (PmP, SmS) and the direct waves (Pg, Sg) for the three events, which are indicative of an essentially identical focal depth. This is a rare example of a sequence of clear and impulsive Pg, PmP, Sg and SmS phases recorded at the same location

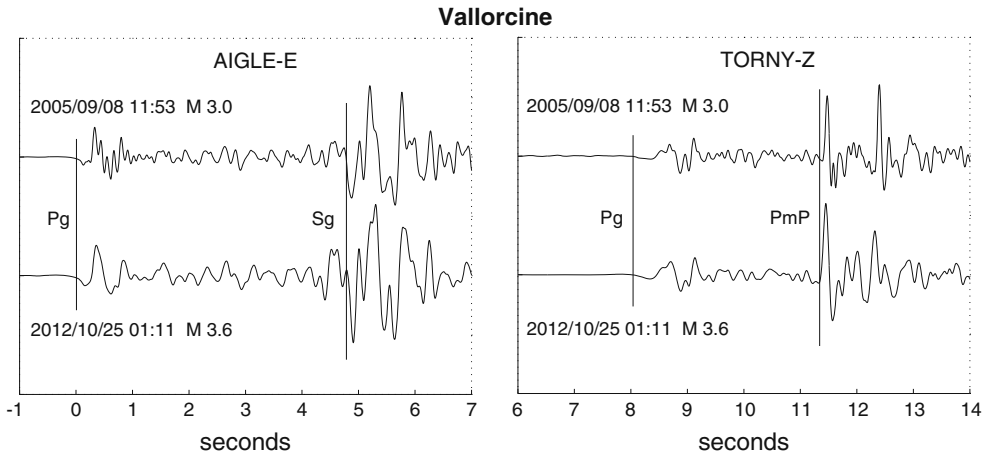


**Fig. 13** Displacement seismograms of the Vallorcine events of 2005/09/08 ($M_L$ 3.0) and 2012/10/25 ($M_L$ 3.6) recorded at stations AIGLE (EW-component, 35 km epicentral distance) and TORNY (Z-component, 82 km epicentral distance). To stabilize the integration and to accentuate differences at high frequency, the signals are filtered with a 1 Hz, 4th order, zero-phase Butterworth high-pass filter and an 8 Hz, 2nd order Butterworth low-pass filter. Because the Pg onsets at TORNY are rather emergent, both sets of seismograms are aligned on the Pg arrival at station AIGLE. Note the high signal similarity as well as the almost identical Sg–Pg arrival-time differences at AIGLE and PmP–Pg arrival-time differences at TORNY for the two events. These similarities are evidence of similar focal mechanisms and almost identical epicenters and focal depths

### *3.2.5 Breithorn*

The $M_L$ 2.9 event of November 28th was located 10 km south of Zermatt (labeled Bre in Fig. 2). The focal depth of 2 km is constrained by P and S-arrivals recorded at epicentral distances of 10 km (station SATI (INGV)) and 20 km (station MMK) and therefore uncertain. Due to the inhomogeneous distribution of first-motion observations, a focal-plane solution could not be reliably determined. The mainshock was followed by 5 aftershocks with $M_L$ 0.7–1.8 in November and December.

### *3.2.6 Santa Maria*

During 2012, a sequence of 15 earthquakes occurred in a region east of Santa Maria (Val Müstair). Based on the routine location and the high similarity of waveforms recorded at station MOSI (Bozen), seven of these events with $M_L$ 1.3–1.9 appear to be co-located (cluster labeled SMa in Fig. 2). The sequence of co-located events started on October 20th and the last event occurred on December 7th. The largest of the events on November 8th was followed by a secondary event separated by about 3 s.

#### 3.2.7 *Seismicity associated with the former Deep Heat Mining project in Basel*

The seismic activity induced by the geothermal project in Basel in 2006 and 2007 (e.g. Deichmann and Ernst 2009; Deichmann and Giardini 2009) continued to decrease over the years 2008–2011, with only one event ($M_L$ 0.6) being recorded by the national network in 2010. In 2012 activity seems to have picked up again: five events, with magnitudes between $M_L = 0.9$–1.2, were strong enough to be recorded by the national broadband network. Master event relocation confirms that the two events of February 26th 2010 and May 20th 2012 as well as the three events which occurred between December 12th and 15th 2012 are located in the same region as the hypocenters of the events which occurred towards the end of 2007 (i.e. above the casing shoe, at the southern periphery of the stimulated rock volume), whereas the event of October 3rd 2012 is located about 400 m below the casing shoe and about 400 m to the east of the main hypocentral cloud. Due to the removal of three of the borehole sensors, relative location uncertainties for the five events of 2012 are about twice as large as for the earlier events. However, with computed standard deviations of 76 m (E–W), 147 m (N–S) and 67 m (Z), the outlier location of the event of October 3rd 2012 is well constrained. The seismic activity in the stimulated rock volume is expected to stay above the natural background level for several years (Bachmann et al. 2011).

## 4 Discussion

In 2012, as in previous years, a large portion of the seismic activity was concentrated in the Valais and the immediately adjacent regions. Routinely calculated focal depths for all but 13 events recorded in 2012 are less than 16 km. All of the deeper hypocenters occurred below the Molasse Basin and the Jura of northern Switzerland and southern Germany, mainly between 7°E and 10°E (e.g. Deichmann 1992; Deichmann et al. 2000a). Overall, the seismic activity in and around Switzerland, in terms of the number of events, was low in 2012. The total number of 13 events with $M_L \geq 2.5$ is substantially below the yearly average of about 24 events over the previous 37 years in this magnitude range. The $M_L$ 4.2 lower-crustal earthquake near Zug, on the other hand, had the largest magnitude since the 2005 Vallorcine earthquake.

**Acknowledgments** Monitoring the seismicity in a small country is not possible without international cooperation. Automatic data exchange in real-time has been implemented with Austria operated by the Zentralanstalt für Meteorologie und Geodynamik in Vienna (ZAMG); with Italy operated by the Istituto Nazionale di Geofisica e Vulcanologia in Rome (INGV), the Istituto di Geofisica, Universita di Genova, the Zivilschutz der Autonomen Provinz Bozen-Südtirol and the Istituto Nazionale di Oceanografia e di Geofisica Sperimentale (OGS) in Trieste; with Germany operated by the Landeserdbebendienst Baden-Württemberg in Freiburg (LED) and the Bundesanstalt für Geowissenschaften und Rohstoffe in Hannover (BGR); and with France operated by the Réseau Sismologique et Géodésique Français (RESIF).

We are also very grateful to our colleagues in the SED seismic network and electronics lab for their relentless efforts in ensuring the continuous reliability of the data acquisition systems and the earthquake monitoring software, and to E. Läderach, S. Brühwiler, and A. Blanchard for administrative and logistic support. We thank Michael Schnellmann and Herwig Müller from Nagra for their support and efforts in installing stations BERGE, EMMET, and STIEG; and Gunter Siddiqi (BFE) and Michael Sonderegger (Sankt Galler Stadtwerke) for their support for the Sankt Gallen seismic monitoring project.

Financial support from the Nationale Genossenschaft für die Lagerung radioaktiver Abfälle, Nagra for the operation of several stations in northern Switzerland is gratefully acknowledged. Installation and operation of the Noville network are funded under a contract with Petrosvibri S.A. We thank the Swiss Federal Office of Energy for the financial support of project GeoBest (http://www.seismo.ethz.ch/research/groups/spec/projects/ProjectGeoBest) that provided the seismic instrumentation for the monitoring network in St. Gallen. Sankt Galler Stadtwerke are gratefully acknowledged for their financial and logistic support in providing the technical infrastructure for the St. Gallen Network, including the 205 m deep monitoring borehole. Financial support for upgrading and operating seismic stations in the Basel region was given by the Kanton Basel Stadt. We thank A. G. Milnes, and two anonymous reviewers for their constructive and helpful reviews.

## References

Bachmann, C. E., Wiemer, S., Woessner, J., & Hainzl, S. (2011). Statistical analysis of the induced Basel 2006 earthquake sequence: Introducing a probability-based monitoring approach for Enhanced Geothermal Systems. *Geophysical Journal International, 186*, 793–807. doi:10.1111/j.1365-246X.2011.05068.x.

Baer, M., Deichmann, N., Ballarin Dolfin, D., Bay, F., Delouis, B., Fäh, D., et al. (1999). Earthquakes in Switzerland and surrounding regions during 1998. *Eclogae Geologicae Helvetiae, 92*, 265–273.

Baer, M., Deichmann, N., Braunmiller, J., Ballarin Dolfin, D., Bay, F., Bernardi, F., et al. (2001). Earthquakes in Switzerland and surrounding regions during 2000. *Eclogae Geologicae Helvetiae, 94*, 253–264.

Baer, M., Deichmann, N., Braunmiller, J., Bernardi, F., Cornou, C., Fäh, D., et al. (2003). Earthquakes in Switzerland and surrounding regions during 2002. *Eclogae Geologicae Helvetiae (Swiss Journal of Geosciences), 96*, 313–324.

Baer, M., Deichmann, N., Braunmiller, J., Clinton, J., Husen, S., Fäh, D., et al. (2007). Earthquakes in Switzerland and surrounding regions during 2006. *Swiss Journal of Geosciences, 100*, 517–528. doi:10.1007/s00015-007-1242-0.

Baer, M., Deichmann, N., Braunmiller, J., Husen, S., Fäh, D., Giardini, D., et al. (2005). Earthquakes in Switzerland and surrounding regions during 2004. *Eclogae Geologicae Helvetiae (Swiss Journal of Geosciences), 98*, 407–418. doi:10.1007/s00015-005-1168-3.

Baer, M., Deichmann, N., Fäh, D., Kradolfer, U., Mayer-Rosa, D., Rüttener, E., et al. (1997). Earthquakes in Switzerland and

surrounding regions during 1996. *Eclogae Geologicae Helvetiae, 90*, 557–567.

Baer, M., & Kradolfer, U. (1987). An automatic phase picker for local and teleseismic events. *Bulletin of the Seismological Society of America, 77*, 1437–1445.

Brune, J. N. (1970). Tectonic stress and the spectra of seismic shear waves from earthquakes. *Journal of Geophysical Research, 75*, 4997–5010.

Brune, J. N. (1971). Correction: Tectonic stress and the spectra of seismic shear waves from earthquakes. *Journal of Geophysical Research, 76*, 5002.

Cauzzi, C. & Clinton, J. (2013). A high- and low-noise model for high-quality strong-motion accelerometer stations. *Earthquake Spectra, 29*, 85–102. doi:10.1193/1.4000107.

Clinton, J., Cauzzi, C., Fäh, D., Michel, C., Zweifel, P., Olivieri, M., Cua, G., Haslinger, F. & Giardini, D. (2011). The current state of strong motion monitoring in Switzerland. In S. Akkar, P. Gülkan, & T. van Eck (Eds.) *earthquake data in engineering seismology*: *Predictive models, data management and networks* (*geotechnical, geological and earthquake engineering*), ISBN 10: 9400701519|2011.

Deichmann, N. (1990). Seismizität der Nordschweiz, 1987–1989, und Auswertung der Erdbebenserien von Günsberg, Läufelfingen und Zeglingen. *Nagra Technischer Bericht, NTB 90-46,* Nagra, Baden.

Deichmann, N. (1992). Structural and rheological implications of lower-crustal earthquakes below northern Switzerland. *Physics of the Earth and Planetary Interiors, 69*, 270–280.

Deichmann, N., Baer, M., Ballarin Dolfin, D., Fäh, D., Flück, P., Kastrup, U., et al. (1998). Earthquakes in Switzerland and surrounding regions during 1997. *Eclogae Geologicae Helvetiae, 91*, 237–246.

Deichmann, N., Baer, M., Braunmiller, J., Ballarin Dolfin, D., Bay, F., Bernardi, F., et al. (2002). Earthquakes in Switzerland and surrounding regions during 2001. *Eclogae Geologicae Helvetiae (Swiss Journal of Geosciences), 95*, 249–261.

Deichmann, N., Baer, M., Braunmiller, J., Ballarin Dolfin, D., Bay, F., Delouis, B., et al. (2000a). Earthquakes in Switzerland and surrounding regions during 1999. *Eclogae Geologicae Helvetiae, 93*, 395–406.

Deichmann, N., Baer, M., Braunmiller, J., Cornou, C., Fäh, D., Giardini, D., et al. (2004). Earthquakes in Switzerland and surrounding regions during 2003. *Eclogae Geologicae Helvetiae (Swiss Journal of Geosciences), 97*, 447–458.

Deichmann, N., Baer, M., Braunmiller, J., Husen, S., Fäh, D., Giardini, D., et al. (2006). Earthquakes in Switzerland and surrounding regions during 2005. *Eclogae Geologicae Helvetiae (Swiss Journal of Geosciences), 99*, 443–452. doi:10.1007/s00015-006-1201-1.

Deichmann, N., Baer, M., Clinton, J., Husen, S., Fäh, D., Giardini, D., et al. (2008). Earthquakes in Switzerland and surrounding regions during 2007. *Swiss Journal of Geosciences, 101*, 659–667. doi:10.1007/s00015-008-1304-y.

Deichmann, N., Ballarin Dolfin, D., Kastrup, U. (2000b). Seismizität der Nord- und Zentralschweiz. *Nagra Technischer Bericht, NTB 00-05,* Nagra, Wettingen.

Deichmann, N., Clinton, J., Husen, S., Edwards, B., Haslinger, F., Fäh, D., et al. (2010). Earthquakes in Switzerland and surrounding regions during 2009. *Swiss Journal of Geosciences, 103*, 535–549. doi:10.1007/s00015-010-0039-8.

Deichmann, N., Clinton, J., Husen, S., Edwards, B., Haslinger, F., Fäh, D., et al. (2011). Earthquakes in Switzerland and surrounding regions during 2010. *Swiss Journal of Geosciences, 104*, 537–547. doi:10.1007/s00015-011-0084-y.

Deichmann, N., Clinton, J., Husen, S., Edwards, B., Haslinger, F., Fäh, D., et al. (2012). Earthquakes in Switzerland and surrounding regions during 2011. *Swiss Journal of Geosciences, 105*, 463–476. doi:10.1007/s00015-012-0116-2.

Deichmann, N., Clinton, J., Husen, S., Haslinger, F., Fäh, D., Giardini, D., et al. (2009). Earthquakes in Switzerland and surrounding regions during 2008. *Swiss Journal of Geosciences, 102*, 505–514. doi:10.1007/s00015-009-1339-8.

Deichmann, N., & Ernst, J. (2009). Earthquake focal mechanisms of the induced seismicity in 2006 and 2007 below Basel (Switzerland). *Swiss Journal of Geosciences, 102*, 457–466. doi:10.1007/s00015-009-1336-y.

Deichmann, N., & Giardini, D. (2009). Earthquakes induced by the stimulation of an enhanced geothermal system below Basel (Switzerland). *Seismological Research Letters, 80*, 784–798. doi:10.1785/gssrl.80.5.784.

Dreger, D. S. (2003). TDMT INV: Time Domain Seismic Moment Tensor INVersion. In W. H. K. Lee, H. Kanamori, P. C. Jennings, & C. Kisslinger (Eds.), *International handbook of earthquake and engineering seismology,* (Part B, p. 1627). London: Academic Press.

Edwards, B., Allmann, B., Fäh, D., & Clinton, J. (2010). Automatic computation of moment magnitudes for small earthquakes and the scaling of local to moment magnitude. *Geophysical Journal International, 183*, 407–420. doi:10.1111/j.1365-246X.2010.04743.x.

Edwards, B., Michel, C., Poggi, V., & Fäh, D. (2013). Determination of site amplification from regional seismicity: Application to the Swiss national seismic networks. *Seismological Research Letters, 84*, 611–621. doi:10.1785/0220120176.

Fäh, D., Giardini, D., Bay, F., Bernardi, F., Braunmiller, J., Deichmann, N., et al. (2003). Earthquake catalogue of Switzerland (ECOS) and the related macroseismic database. *Eclogae Geologicae Helvetiae (Swiss Journal of Geosciences), 96*, 219–236.

Fréchet, J., Thouvenot, F., Frogneux, M., Deichmann, N., & Cara, M. (2010). The $M_w$ 4.5 Vallorcine (French Alps) earthquake of 8 September 2005 and its complex aftershock sequence. *Journal of Seismology, 15*, 43–58. doi:10.1007/s10950-010-9205-8.

Giardini, D., Wiemer, S., Fäh, D., Deichmann, N., Sellami, S., Jenni, S. & the Hazard Team of the Swiss Seismological Service (2004). Seismic Hazard Assessment 2004. *Swiss Seismological Service*.

Hanka, W., Saul, J., Weber, B., Becker, J., Harjadi, P., Fauzi; GITEWS Seismology Group (2010). Real-time earthquake monitoring for tsunami warning in the Indian Ocean and beyond. *Natural Hazards and Earth System Sciences, 10*, 2611–2622, doi:10.5194/nhess-10-2611-2010.

Husen, S., Bachmann, C., & Giardini, D. (2007). Locally triggered seismicity in the central Swiss Alps following the large rainfall event of August 2005. *Geophysical Journal International, 171*, 1126–1134. doi:10.1111/j.1365-246X.2007.03561.x.

Husen, S., Kissling, E., Deichmann, N., Wiemer, S., Giardini, D., & Baer, M. (2003). Probabilistic earthquake location in complex three-dimensional velocity models: Application to Switzerland. *Journal of Geophysical Research, 108*, 2077–2096.

Husen, S., Kissling, E., & von Deschwanden, A. (2011). Induced seismicity during the construction of the Gotthard Base Tunnel, Switzerland: Hypocenter locations and source dimensions. *Journal of Seismology,*. doi:10.1007/s10950-011-9261-8.

Kastrup, U., Zoback M.-L., Deichmann, N., Evans, K., Giardini, D., & Michael, A.J. (2004). Stress field variations in the Swiss Alps and the northern Alpine foreland derived from inversion of fault plane solutions. *Journal of Geophysical Research, 109*. doi:10.1029/2003JB002550B01402.

Kastrup, U., Deichmann, N., Fröhlich, A., & Giardini, D. (2007). Evidence for an active fault below the north-western Alpine foreland of Switzerland. *Geophysical Journal International, 169*, 1273–1288. doi:10.1111/j.1365-264X.2007.03413.x.

Kradolfer, U. & Mayer-Rosa, D. (1988). Attenuation of seismic waves in Switzerland. In *Recent seismological investigations in Europe*. *Proceedings of the XIX General Assembly of the ESC, Moscow* (pp. 481–488).

Lomax, A., Virieux, J., Volant, P., & Thierry-Berge, C. (2000). Probabilistic earthquake location in 3D and layered models. In C. H. Thurber & N. Rabinowitz (Eds.), *Advances in seismic event location* (pp. 101–134). London: Kluwer Academic Publishers.

Marschall, I., Deichmann, N., & Marone, F. (2013). Earthquake focal mechanisms and stress orientations in the eastern Swiss Alps. *Swiss Journal of Geosciences, 106*, 79–90. doi:10.1007/s00015-013-0129-5.

Nanjo, K. Z., Schorlemmer, D., Woessner, J., Wiemer, S., & Giardini, D. (2010). Earthquake detection capability of the Swiss Seismic Network. *Geophysical Journal International, 181*, 1713–1724. doi:10.1111/j.1365-246X.2010.04593.x.

Pavoni, N. (1977). Erdbeben im Gebiet der Schweiz. *Eclogae Geologicae Helvetiae, 70*, 351–370.

Pavoni, N., Maurer, H., Roth, P., Deichmann, N. (1997). Seismicity and seismotectonics of the Swiss Alps. In *Deep structure of the Swiss Alps, results of NRP 20* (pp. 241–250). Basel: Birkhäuser.

Pavoni, N. & Roth, P. (1990). Seismicity and seismotectonics of the Swiss Alps. Results of microearthquake investigations 1983–1988. In F. Roure, P. Heitzmann & R. Polino (Eds.), *Deep Structure of the Alps,* Mémoire de la Societé geologique de France, Paris (Vol. 156, pp. 129–134.

Poggi, V., Edwards, B., & Fäh, D. (2011). Derivation of a reference shear-wave velocity model from empirical site amplification. *Bulletin of the Seismological Society of America, 101*, 258–274.

Rüttener, E. (1995). Earthquake hazard estimation for Switzerland. *Matérials Géologie Suisse, Geophysique,* Nr. 29, Schweizerische Geophysikalische Kommission, ETH-Zürich.

Rüttener, E., Eogozcue, J., Mayer-Rosa, D., & Mueller, S. (1996). Bayesian estimation of seismic hazard for two sites in Switzerland. *Natural Hazards, 14*, 165–178.

Sägesser, R., & Mayer-Rosa, D. (1978). Erdbebengefährdung in der Schweiz. *Schweizerische Bauzeitung, 78*, 3–18.

Wagner, M., Kissling, E., & Husen, S. (2012). Combining controlled-source seismology and local earthquake tomography to derive a 3-D crustal model of the western Alpine region. *Geophysical Journal International, 191*, 789–802. doi:10.1111/j.1365-246X.2012.05655.x.

Wiemer, S., Giardini, D., Fäh, D., Deichmann, N., & Sellami, S. (2009). Probabilistic seismic hazard assessment of Switzerland: Best estimates and uncertainties. *Journal of Seismology, 13*, 449–478. doi:10.1007/s10950-008-9138-7.